HHS Public Access

Author manuscript

Adv Drug Deliv Rev. Author manuscript; available in PMC 2018 June 27.

Published in final edited form as:

Adv Drug Deliv Rev. 2018 March 01; 127: 106–118. doi:10.1016/j.addr.2018.01.015.

Polymeric microneedles for transdermal protein delivery☆

Yanqi Ye[a,b], **Jicheng Yu**[a,b], **Di Wen**[a,b], **Anna R. Kahkoska**[c], and **Zhen Gu**[a,b,c,*]

[a]Joint Department of Biomedical Engineering, University of North Carolina at Chapel Hill and North Carolina State University, Raleigh, NC 27695, USA

[b]Division of Pharmacoengineering and Molecular Pharmaceutics, Eshelman School of Pharmacy, University of North Carolina at Chapel Hill, Chapel Hill, NC 27599, USA

[c]Department of Medicine, University of North Carolina School of Medicine, Chapel Hill, NC 27599, USA

Abstract

The intrinsic properties of therapeutic proteins generally present a major impediment for transdermal delivery, including their relatively large molecule size and susceptibility to degradation. One solution is to utilize microneedles (MNs), which are capable of painlessly traversing the stratum corneum and directly translocating protein drugs into the systematic circulation. MNs can be designed to incorporate appropriate structural materials as well as therapeutics or formulations with tailored physicochemical properties. This platform technique has been applied to deliver drugs both locally and systemically in applications ranging from vaccination to diabetes and cancer therapy. This review surveys the current design and use of polymeric MNs for transdermal protein delivery. The clinical potential and future translation of MNs are also discussed.

Keywords

Drug delivery; Transdermal; Microneedle; Protein delivery; Vaccine

1. Introduction

Transdermal drug delivery offers a clinical superiority over traditional, invasive injections. As compared to oral delivery, protein drug transportation across the skin avoids the hepatic first-pass extraction and is delivered to the systematic circulation at a pharmacologically relevant rate [1,2]. However, the clinical application of transdermal delivery had been limited to lipophilic drugs with a molecular weight less than 500 Da [3–5] until the emergence of polymeric microneedles (MNs), which provides a broad and versatile platform to overcome the challenges of the skin barrier for macromolecular drugs. In this technique, arrays of microscopic needles with lengths ranging from 50 to 900 μm are designed to painlessly transverse the stratum corneum and penetrate the epidermis layer at a

☆This review is part of the *Advanced Drug Delivery Reviews* theme issue on “Skin-Associated Drug Delivery”.

*Corresponding author at: Joint Department of Biomedical Engineering, University of North Carolina at Chapel Hill and North Carolina State University, Raleigh, NC 27695, USA. zgu@email.unc.edu (Z. Gu).

predetermined depth, thereby avoiding the stimulation of the nerve endings [6–9], improving treatment compliance and patient acceptability. Drugs exposed to the epidermis/dermis layers of the skin can be rapidly absorbed through both diffusion and lymph-mediated uptake in the regional capillaries and lymphatic networks [10–12]. In addition, the skin acts as a highly active organ from an immunological perspective [13–16]. Enhanced local immune responses can also be achieved *via* MN administration route due to the abundance of resident antigen-presenting cells (APCs) including Langerhans cells and subsets of T lymphocytes in the dermal layer [17–20]. A dose-sparing effect of MN vaccine has been observed compared to the traditional intramuscular immunization, eliciting commensurate humoral, cellular and mucosal immune responses [21,22].

To date, MNs have been applied in the delivery of distinct cargoes, from native protein therapeutics to nano- or microparticle (MP)-based formulations [12,23–28]. Of these models, biocompatible polymer-based MN devices have been leveraged to address several issues in transdermal protein delivery [7,29–32]. Compared to the MNs developed in the early years, such as the silicon or metal MNs, the polymeric MNs can eliminate the sharp biohazard wastes, avoid deleterious effects on drug stability and allow the drug loading to be readily tailored [33–35]. Encapsulating proteins in the polymeric matrix provides the opportunity for long-term maintenance of bioactive protein in a dried state without the cold chain requirement, thereby minimizing the costs and restrictions of transportation [36–38]. Further adjustment of the formulation facilitates optimization of the physiochemical properties and spatiotemporal release profiles of the drugs over hours to days [39–42]. This review summarizes the delivery of proteins through representative types of polymeric MNs for a variety of applications, discusses the current state of the field, and highlights the future potential of polymeric MNs for protein delivery. The challenges for clinical translation are also discussed in the end.

2. Types of delivered protein

Proteins play functionally distinct and dynamic roles in the body, such as enzymatic catalysis, cellular regulation, biological scaffold and molecular transportation [43]. The clinical development of protein drugs is estimated to expedite compared to small-molecule drugs and other macromolecular therapeutics [44,45]. Protein drugs can be used to directly replace the dysfunctional endogenous protein and are applicable to a variety of cancer treatments, vaccinations and therapies for genetic disorders [46–48]. Additionally, because of the specific functionality and structural hierarchy, therapeutic proteins mitigate the side-effects of interference with the biological system [49,50]. However, the intrinsic properties of the therapeutic protein also pose significant challenges for the full potential of its transdermal delivery [49,51,52]. For example, protein denaturation during administration and/or subsequent storage process can result in limited therapeutic efficiency, altered regulatory response and impaired vaccination efficiency [53–55]. Besides the maintenance of bioactivity, the therapeutic efficacy is also impacted by the drug absorption efficiency, which is determined by the chemical properties, the structural differences of the drug and the physiological conditions of the skin [56,57]. Cellular permeability related to the molecular size is also critical: proteins/peptides of less than approximately 5000 Da could transverse the skin layer and blood capillaries easily compared to those with the molecular weight

greater than 20,000 Da [54,58,59]. In addition, it has been suggested that the hydrolytic attacks by proteases in the skin and blood/lymphatic network may also limit the bioavailability of MN-administered proteins [60]. Therefore, appropriate materials and formulations to preserve the protein integrity and improve the delivery efficiency are highly desirable for this form of therapy [61,62]. In this section, typical protein therapeutics and their properties associated with MN-mediated delivery approaches are briefly surveyed.

2.1. Proteins with enzymatic or regulatory activity

Effective delivery of proteins with enzymatic or regulatory activity has been developed using MN technology, including insulin, desmopressin, erythropoietin, lysozyme, glucagon, glucagon-like peptide-1 (GLP-1), parathyroid hormone (PTH), growth hormone and etanercept [6,42,63]. The selections of materials and formulation to preserve the protein drug stability remain to be a challenge, particularly in large-scale storage schemes and in production chains for clinical use. Donnelly et al. investigated the thermal stability of the loaded protein and found that the high melting temperature (160 °C) of molten galactose during MN fabrication process resulted in substantial loss of incorporated 5-aminolevulinic acid and bovine serum albumin (BSA) [64]. Researchers further measured the effect of thermal exposure (135 °C) of BSA in melted poly(lactide-*co*-glycolide acid) (PLGA) during the fabrication process and found little difference in the circular dichroism spectra comparing the ratio of α-helix/β-sheet to the native BSA [5]. Moreover, it was demonstrated that the proteins in the solid state had increased stability during thermal processing than the proteins in the aqueous solution [5,65]. Carboxymethylcellulose (CMC)-based MNs have successfully incorporated a variety of protein compounds, including BSA and lysozyme [23], which were found to be stable after two months of storage. Carbohydrate melt-based MNs, which involve casting the solution into a mold followed by evaporation at 37 °C, have also been developed [23]. For example, recombinant human growth hormone (rhGH) and insulin were stably embedded in MN patches and stored at room temperature for 15 months and one month, respectively [42,66]. PTH was coated onto MNs and retained most of its bioactivity after up to 18 months at room temperature and 60% humidity [67].

2.2. Antibodies

Monoclonal antibodies leverage the antigen recognition capability of immunoglobulin sites and the receptor-binding domains of protein ligands to target certain cells and regulate the immune system [59,68,69]. Their effectiveness has been proven for a wide spectrum of diagnostic and therapeutic applications [70–74]. For example, immune checkpoint blockade therapy has recently shown promise in cancer immunotherapy to overcome the immunosuppressive nature of tumors. Strategy of local delivery, rather than systemic administration, is one approach to address the immune-related adverse events by alleviating the overstimulation of self-reactive T cells. Therefore, researchers have investigated the applicability of MN-mediated transdermal technique to deliver monoclonal antibodies [75,76].

Potential complications of antibody delivery may also arise from the deactivation of protein, including loss of efficacy, risks of immunogenicity and immune complex hypersensitivity [77–79]. It is critical that the stability of antibodies in MN formulations is well preserved to

avoid such undesirable effects. Properties of antibodies need to be characterized including targeting specificity, molecular structure and antigen affinity [80]. To this end, studies have shown that more than 80% of monoclonal immunoglobulin G (IgG) was recovered with stable tertiary conformation after the dissolution of hyaluronan (HA)-based dissolvable MNs [81]. Further, no formations of IgG aggregation or HA/IgG complexes were detected during the MN preparation process. Studies have also indicated that human IgG delivered through hairless rat skin remained mostly localized in and around the microchannels created by the maltose MNs [75]. The skin retention capability of the active IgG was influenced by factors including the MN array size, the length of the MNs and macromolecule concentration. Other factors such as biocompatibility, availability and production cost also need to be considered.

2.3. Vaccines

Current vaccines are generally limited to subcutaneous injection [82–85], while MNs loaded with antigenic therapeutics have recently been studied to induce significant antibody- and cell-mediated immune responses [22,86,87]. The merits of MN vaccines include the effective antigen presentation to skin-resident dendritic cells (DCs) which often enables stronger topical immunization than soluble antigens *via* intramuscular injection [88–90]. In addition, a variety of MN matrix biomaterials could also serve as adjuvants to enhance the immune responses due to their intrinsic immunogenicity. For instance, PLGA could promote antigen-specific antibody and type 2 T helper (Th2) cell-dependent humoral responses against co-delivered antigen [91]; HA is associated with a key role in regulatory functions of T cells in the peripheral blood [92].

Currently, availability of the vaccine is often limited by their reliance on the low-temperature storage and transportation [93]. A better understanding of the vaccine stability throughout the fabrication, storage and administration process is essential for the future optimization [94]. Appropriate formulation methods using MN patch preserve the long-term antigen immunogenicity and allow flexible storage conditions [95]. To assess the effect of the coating formulation to the stability of viral proteins, Zhu et al. suspended the viral proteins in a coating solution and found the experimental responses were comparable with the control groups in terms of antibody production [96]. A dissolvable MN patch fabricated from CMC and trehalose was used to deliver influenza vaccine. It was demonstrated that the MN injection was associated with improved viral protein stability and protective immunity compared to intramuscular injection of the solution-based vaccine [97]. At the same time, a stabilizing effect of trehalose on the hemagglutinin activity of inactivated influenza virus was also observed after being coated onto the MN surface [98]. A recombinant protective antigen was also administered using dissolvable MNs and exhibited a comparable immune response to intramuscular or intradermal injection in rats [99]. These results suggested that the appropriate drying and coating procedure could tune the glass transition temperature below the storage temperature in order to prevent the crystallization of vaccine formulation, leading to its long-term stability [100]. Ovalbumin (OVA) is a model protein with unique lymph node-targeting capability that has often been used to evaluate the performance of MNs for immunization. It was found that mice administered with OVA-loaded MNs induced elevated frequency of interferon-γ (IFN-γ)-secreting CD4+ T cells and enhanced level of serum IgG compared to intradermal immunization [11,101]. The treatment efficacy of the

MN approach has been tested in large animal subjects as well, including non-human primates by Irvine's group [102]. MNs made of poly-L-lactide (PLA) were fabricated through melt-molding and coated with Adenovirus Type 5 (Ad5) vectors in a 5% aqueous sucrose matrix. To evaluate the functional immunogenicity of MN-based adenovirus delivery, the patches were applied to the shaved deltoid skin of anesthetized macaques twice. This delivery method induced strong cellular and humoral adenovirus-specific vaccination in macaques equivalent to the traditional intramuscular injection [102]. In a recent study, an MN patch containing sucrose and CMC was formulated to encapsulate the standard dose of measles vaccine and was tested in rhesus macaques [103]. The researchers demonstrated that the macaques responded to MN vaccination with equivalent neutralizing antibody titers compared to the conventional subcutaneous injection.

3. Representative types of polymeric MN

The typical design parameters to be considered in the selection of polymeric matrix include biocompatibility, biodegradability, solubility and mechanical properties. Based on the available materials and formulations, the construction of an MN delivery system can be achieved *via* several main strategies as illustrated in Fig. 1. The first approach relies on the coating of the polymer and drug formulation onto the solid MNs and dissolution of the coating shell to facilitate drug release (Fig. 1A). The second approach utilizes the incorporation of payloads into the matrix of the dissolvable polymeric MNs (Fig. 1B). In this method, delivery efficiency is determined by the rate of polymer dissolution following the insertion into the skin. The third approach allows for the delivery of payloads *via* passive diffusion or degradation of the polymeric matrix (Fig. 1C). When combined with secondary encapsulation techniques such as the micro- and nano-formulations, the drug release can be tuned in a bioresponsive manner, which is described as the fourth approach here (Fig. 1D). Next, each of these representative MN types MNs will be discussed in details.

3.1. Coated MN

The first generation of MN therapy relies on the increased skin permeability after perforation by the solid MNs in combination with topical application of active molecules [93,104]. However, it has often been limited by low delivery efficiency, a lack of precise dosing and complex administration procedures [7,33]. From a safety perspective, those microchannels in the skin after needle removal cause exposure to toxic agents such as pathogenic microorganism and impose infection-associated risks [105]. One way to optimize this approach is to coat the drug payload directly onto the surface of solid MNs. A variety of strategies have been developed for coating and drying drug molecules onto the surface of MNs, including dip-coating, casting and deposition techniques [106,107]. Furthermore, the drug can be deposited at specific skin depth, determined by the dimensions of the MN and the application method [108].

Peter et al. reported the preparation of a sucrose-coated titanium MN system for transdermal delivery of recombinant human erythropoietin alfa (EPO). The researchers evaluated the preclinical pharmacokinetic performance of this coating formulation [109]. Cormier et al. prepared a titanium MN array coated with 82 μg desmopressin on the MN surface for the

treatment of enuresis [110]. Drug utilization to hairless guinea pigs was calculated to be 85%, while the desmopressin was readily released following the dissolution of the coating polymer polysorbate 20. Coated MN systems that incorporate the antigenic proteins are particularly effective as an intradermal vaccination approach, providing striking improvements in immune response and minimum patient compromise compared to intramuscular injection [96,111,112]. This approach has been employed successfully in immunization studies of OVA, H3N2 influenza antigen, inactivated influenza virus and Hepatitis C DNA vaccine, with doses ranging between 0.4 and 10 μg [113]. Specifically, Matriano et al. used 1 μg of OVA pre-coated MN arrays with 300 μm high needles made of titanium and demonstrated a 100-fold increase in the immune response compared to intramuscular route [114]. Zhu et al. assessed the efficacy of CMC-coated metal MNs (500 μm) for antigen delivery using inactivated influenza viral proteins [96]. Within 5 min of insertion time, up to 90% of the coated viral proteins were deposited inside the skin of a BALB/c mouse model. Moreover, the delivery of antigen protein *via* MNs induced robust antibody production that was comparable to that induced by conventional intramuscular immunization. Mutwiri et al. selected polyphosphazene polyelectrolyte (PCPP) as the polymeric matrix with fluorescein isothiocyanate (FITC) labeled BSA as a model protein for the study [115]. *In vitro* and *in vivo* studies were conducted to investigate the MN capability of penetrating the stratum corneum and the dynamics of the release profile of the model protein. The results showed the complete dissolution of the polymer accompanied with the release of the total amount of protein in 15 min in the porcine cadaver skin of a 4-week-old pig.

Furthermore, a layer-by-layer assembled polyelectrolyte multilayers (PEMs) structure was reported by DeMuth et al. [116]. This technique allowed the researchers to control the film thickness and drug dosage for tunable stabilizing and releasing purposes. Specifically, liposomes loaded with OVA, an adjuvant, and a fluorescent tracer were co-encapsulated inside the PEMs. The OVA was taken up by the APCs presented abundantly in the cutaneous tissue after the transcutaneous vaccination. This resulted in significantly higher levels of anti-OVA IgG titers in the serum and enhanced humoral immune response (Fig. 2). Irvine and coworkers tested the efficacy of PEMs-coated PLGA MNs for transporting antigens into the skin, targeting epidermal and dermal APCs [117]. They used a biodegradable polymer poly(*β*-amino esters) (PBAEs) to encapsulate protein antigen-loaded lipid nanovesicles [118]. Multilayers of MN surface were assembled to deliver the protein payload into the dorsal ear or flank skin of mice *via* the MN administration. Subsequent confocal imaging revealed that the PBAE multilayers were degraded in the treated tissue over one day period, and the dispersed nanovesicles were continuously taken up by the APCs. More than 10-fold higher serum IgG titers were observed compared to the free OVA injection, suggesting that this system could be used as a platform for vaccination against emerging infectious pathogens [117]. In addition, Prausnitz and coworkers developed another technique of layer-by-layer deposition of polyelectrolytes, which was used to coat bovine pancreatic ribonuclease A onto the stainless steel MNs [119]. The release of the protein drug was mediated by the hydrolytic degradation of the coating layer after the insertion into the porcine cadaver skin with a depth of around 500 μm. More recently, MNs loaded with a conserved human melanoma antigen with assembled PEMs structures were developed [120].

The immunized mice showed expansion of tumor-specific T cells and potent memory recall responses. A potential limitation of this approach, however, is that such MNs often leave behind biohazardous waste after use, raising potential concerns about needle-based injuries without special disposal protocols. The effectiveness of coated MN-based delivery is also limited by the surface area of the MN matrix and the adhesion to the drug-loaded polymer film, resulting in variability in drug loading [30,96,104,110].

3.2. Dissolvable MN

Dissolvable MNs are designed to encapsulate drug within the soluble polymeric matrix and become fully dissolved upon insertion into the skin. The associated therapeutic duration has been reported to vary widely, ranging from hours to days, and is largely dependent on the dissolution kinetics of the selected polymer and administration time of MNs [121,122]. Regarding the protein stability, it requires the mild conditions for micromolding to maintain the bioactivity of protein drugs [26]. Typical dissolvable polymers used for preparing MNs include CMC [42], maltose [28,123], chitosan [124] and polyvinyl alcohol (PVA) [125].

Maltose-based MNs can fully dissolve in the human skin within 10 min after insertion [126]. However, these MNs often require the fabrication temperature to be above 100 °C to effectively transform the maltose into the glassy phase [123]. Such a high fabrication temperature is generally not suitable for protein-associated formulations. In addition, it is difficult to control the mechanical properties of the MNs, due to the properties of the disaccharide maltose under high humidity conditions. New fabrication techniques have also been developed to address the thermal challenges of melting fabrication process. For example, Jung et al. invented a dissolvable MN fabrication technique by directly applying the droplet-born air blowing to the polymer droplet to solidify the MN shape, thereby providing benign fabrication conditions for the delivery of insulin [127]. The high 96.6 ± 2.4% bioavailability data was confirmed by the regulated blood glucose (BG) levels in the experimental type 1 diabetic mice. Martin et al. tested a low-temperature vacuum-forming methodology, demonstrating that MNs could be fabricated from a dehydrated sugar mixture of trehalose anhydrous (TRA), trehalose dihydrate (TRD), sucrose and maltose [128]. The feasibility of dextran MNs prepared by forming thread with polypropylene has been studied in rats. The plasma levels of rhGH in rats reached peak levels 1 h following MN administration and were shown to have a comparable profile with the intravenously injected rhGH solution [129]. The maximum serum drug concentration was achieved in a dose-dependent manner based on the drug loading capacity of the MNs.

Polymers with high solubility are associated with rapid swelling and dissociation of the polymer chain network, thereby accelerating the drug diffusion upon MN insertion [11]. Migalska et al. described dissolvable MNs prepared from an aqueous blended solution of poly (methylvinylether maleic anhydride) (PMVE/MA) for insulin delivery, showing a significant reduction of BG levels in diabetic mice upon treatment [130]. Brouwstra et al. developed HA-based MNs for the delivery of active monoclonal IgG [81]. HA is a polyanionic disaccharide that is ubiquitously present in the body and has been approved by US Food and Drug Administration (FDA) as a dermal filler [92]. MNs containing 2% or 10% (w/w) of monoclonal IgG were successfully prepared using the micromolding method.

Upon dissolution of MNs, 80% of the incorporated IgG was recovered and its tertiary conformation was insignificantly affected by the preparation process. HA and IgG were found to localize within the skin 10 min after the needle insertion [81]. MNs made of other biocompatible materials such as polyvinylpyrrolidone could also be used to deliver inactivated influenza virus vaccine in a few minutes [12]. The length of MNs was approximately 650 μm, corresponding to the penetration depth of around 200 μm into the porcine cadaver skin *ex vivo*. When the MNs were administrated to the mice *in vivo*, MN dissolved quickly and deposited drug loading into the epidermis. As a result, the mice immunized with MN showed similar levels of serum influenza-specific IgG titer and isotypes, IgG1 and IgG2a (Fig. 3). It was further observed that a 1000-fold higher extent of lung virus clearance was associated with the MN vaccine *versus* intramuscular immunization. In addition, Donnelly and co-workers formulated dissolvable PMVE/MA-based polymeric MN arrays to encapsulate recombinant HIV antigens [131]. The MNs treated-subjects elicited a significantly higher degree of antigen-specific immunity including type 1 T helper (Th1)/Th2 profile, Th2 polarization as well as immunoglobulin A (IgA) levels which surpassed the mucosal vaccination method.

Physiochemical properties of the matrix material should be carefully evaluated to achieve ideal mechanical properties and drug release dynamics. For example, researchers formed dissolvable MNs *via* polymerization of a liquid monomer vinyl pyrrolidone and inactivated hemaglutinin antigen [12]. The researchers further characterized the dissolving kinetics and showed that MN deposited around 34%, 63% and 83% of the total polymer in the porcine skin after 5, 10 and 15 min, respectively. Chen et al. encapsulated insulin into a dissolvable starch/gelatin MN patch that could rapidly dissolve in the interstitial fluid of the skin after insertion [132]. In this system, gelatin was selected as one of the matrix material because of its biodegradability, biocompatibility, non-immunogenicity and film-forming ability. Blended with starch, it formed a durable and strong composite suitable for MN matrix. Moreover, after storage at 25 or 37 °C for one month, the relative bioavailability of insulin was measured to be greater than 90%. The reduced BG levels demonstrated stable encapsulation of bioactive macromolecules in MNs (Fig. 4). The assembled layers were developed to deliver multiple payloads within the one array and to avoid excess payload waste on the surface of the skin. Takada et al. reported two-layered dissolvable MNs for the delivery of rhGH and desmopressin in the rat abdominal skin. The proteins were co-encapsulated in the MNs composed of water-soluble biopolymers chondroitin sulfate or dextran [133]. Similarly, a two-layered MN array was reported with accumulated PLGA particles at the needle tips and dissolving PVA polymer throughout the needle body for maximum drug deposition in the skin [134].

3.3. Degradable MN

A variety of therapeutic proteins require continuous release over a pre-determined period to maintain a constant therapeutic dose [8]. To achieve this, transdermal MN patches made of biodegradable polymers have been developed for the sustained release of payload upon hydrolysis of the polymeric matrix [5]. The release profile of the protein drug depends on the degradation of the polymer and the diffusion of the protein from the MNs, which in turn

can be controlled by selection of polymers with appropriate molecular weight and degradability [124].

Hammond and coworkers reported the utilization of silk fibroin/poly(acrylic acid) (PAA) composite to fabricate microstructures with high biocompatibility and biodegradability [135,136]. The MN patch was composed of a silk tip supported on a PAA pedestal base. The benign aqueous-based micromolding fabrication method, room temperature condition and atmospheric pressure, helped preserve the activity of temperature-labile therapeutics such as peptides, antibiotics and vaccines. Variation in the strength of antigen-specific T-cell responses was dependent on the programmed release of the model drug OVA, which was achieved by adjusting the post-processing conditions of the MN structures (Fig. 5). Other stretchable devices with biodegradable MNs have been developed for insulin delivery. The crosslinked HA matrix efficiently protected the protein from enzymatic degradation and exhibited sustained release efficiency after each stretching trigger (10 cycles of stretching with strain level of 50%). The pulsatile reduction of BG levels was observed upon the three stretching events with four hour-intervals [137]. Recently, phase-transition MNs developed by Yang et al. were able to release insulin by converting the MN material form hard glassy state to hydrogel state upon insertion into the skin [138]. The needles made of PVA were cross-linked to avoid dissolution in the dermis layer, allowing the entire needle to be completely withdrawn from the skin after drug release. Moreover, a transdermal cancer vaccine patch made of the same crosslinked HA materials has been demonstrated by Ye et al. [139]. The MNs consisted of whole tumor lysate from B16F10 melanoma with melanin as well as immunostimulatory agent granulocyte-macrophage colony-stimulating factor (GM-CSF). The content of melanin provided a photosensitizer that promoted immune cells recruitment and activation *via* localized near-infrared light irradiation and subsequent heat generation. Together, this vaccine induced the antitumor effect in both prophylactic and established B16F10 melanoma tumor models and led to enhanced survival [139]. Factors to be considered during the design of immunotherapeutic MN patches include the incorporation of immune-stimulatory adjuvant, appropriate temporal or spatial control over immune cell activation and co-treatments to overcome the immune evasion.

Compared with bulk formulations, substantial efforts have been aimed to incorporate functionalized moieties within the nano/microformulation designs for therapeutic proteins. Drug-loaded MPs have been exploited for prolonged and responsive release from polymeric MNs. Using this approach, the release kinetics of a model protein drug BSA has been shown to range from hours to months, controlled by the formulation of CMC and polylactide acid (PLA) MPs encapsulated within the PLGA MNs [5]. After incubation in phosphate-buffered saline (PBS) for 9 h, MNs showed minimum morphology changes caused by polymer dissolution. The release was also simulated by the diffusion-based Higuchi equation. Zaric et al. found that PLGA nanoparticles (NPs) containing chicken OVA could be successfully delivered by MN arrays into the skin *in situ* [140]. The skin APCs were able to carry the NPs to cutaneous draining lymph nodes *via* the afferent lymphatics. Moreover, those antigens were found to be more efficiently cross-presented *via* major histocompatibility complex (MHC) class I molecules to $CD8^+$ T cells than soluble antigens, allowing the simultaneous stimulations of OVA-specific IFN-γ positive CD4+ and CD8+ T cells in a murine model. The system is applicable to para-influenza infection and melanoma

vaccination (Fig. 6). Additionally, Park and coworkers reported swelling MNs composed of a network of depot hydrogel MPs for topical delivery of drugs through the hydrogel volume expansion in the skin [141]. These MNs were fabricated by micromolding of PLGA matrix containing 53% (v/v) poly-*N*-isopropylacrylamide (PNIPAAm) MPs. Implanting biodegradable polymeric MNs with hydrogel particles promised a long-term delivery of drugs over a few days to a few months. This implantation was described as a two-step process. First, all MNs were mechanically broken after insertion in the skin due to the morphological change of particles. Drug release was then achieved by drug diffusion and degradation of the PLGA MNs.

3.4. Bioresponsive MN

Bioresponsive MNs can be triggered to release protein therapeutics in response to the physiological signals [52,142,143]. This platform often integrates the polymeric matrix only, or together with the sub-micrometer- or nanometer-sized particles in which a therapeutic protein of interest is encapsulated [144–146]. The MN matrix or embedded carriers can undergo dissociation or degradation under certain physiological conditions such as variations in pH, glucose, reactive oxygen species and enzymes [146–148]. It offers opportunities for on-demand release of payload in a relatively precise manner [149,150].

For example, Yu et al. invented a transdermal system composed of crosslinked HA matrix containing glucose-responsive vesicles (GRVs) as a “smart insulin patch”, representing a painless and disposable modality [41]. Drug delivery occurred as follows: in the presence of high BG, glucose oxidase (GOx) catalyzed glucose oxidation by consuming the dissolved oxygen in the body fluid, resulting in a localized hypoxic environment. The resulting bioreduction product of 2-nitroimidazole conjugated HA was water-soluble, leading to the rapid dissociation of GRVs and subsequent release of insulin. *In vivo*, the transcutaneous MN containing the GRVs caused BG levels in the chemically-induced diabetic mice to quickly decline to around 200 mg/dL within half an hour after treatment. Critically, the use of an additional patch could further prolong the treatment period without the risks of hypoglycemia. The treated skin recovered within 6 h with no obvious inflammation, indicating the biocompatibility of the insulin delivery device (Fig. 7). Furthermore, Ye et al. described an innovative MN-based strategy for the glucose-responsive regulation of insulin secretion from exogenous pancreatic β-cell lines without implantation [151]. The MNs encapsulated synthetic glucose-responsive nanovesicles, which were used to amplify the glucose signals through sequential enzymatic reactions. The subsequently amplified glucose signal within the MN microenvironment was able to trigger insulin secretion from the pancreatic β-cell capsules positioned on the base of the patch. One such MN patch was shown to quickly reduce blood sugar levels of streptozotocin (STZ)-induced type 1 diabetic mice and maintain reduced glucose levels for over 10 h. Such bioresponsive system was constructed to leverage the byproduct of glucose oxidation to facilitate insulin release from the MNs [152]. In addition, Yu et al. have also designed hypoxia and H_2O_2 dual-sensitive vesicles integrated with MNs for enhanced glucose-responsive insulin delivery [153]. Diblock copolymers consisting of poly(ethylene glycol) (PEG) and 2-nitroimidazole-modified polyserine were utilized to formulate the dual-sensitive nanovesicles. Rapid oxygen consumption and H_2O_2 generation upon contacting with glucose contributed to the

increased water-solubility of such copolymer, leading to the dissociation and release of insulin. This patch could effectively regulate BG levels in diabetic mice for 10 h and was associated with minimal skin inflammation. Most recently, Chen and coworkers reported MN-array patches loaded with mineralized particle formula to deliver exendin-4 (Ex4) while avoiding the leakage of GOx for long-term type 2 diabetes treatments. Using diabetic C57BL/6 db/db mice as a model, they demonstrated the crosslinked alginate patch loaded with 300 μg Ex4 could control the BG of mice for 5 to 6 days. Furthermore, by integrating the mineralized particles, the failure force of the needles was significantly increased to facilitate skin penetration [63].

With a pH ranging from 4.2–5.6 across the stratum corneum, the local environment is mildly acidic and can act as a significant physiological trigger for drug release from transdermal patches [154]. Kim et al. developed a pH-responsive PEM assembly composed of alternating heparin and albumin films to form a polydopamine (pDA)-coated MN patch [155]. Due to its charge reversal characteristics, albumin was employed to facilitate the pH-dependent hydrolysis of cationic PEM assembly layer. In another example of pH-responsive MNs, poly (vinylpyrrolidinone) (PVP) MNs were composed of hollow PLGA MPs, encapsulating red-fluorescent dye Cy5 as a model drug and a pH-sensitive element sodium bicarbonate ($NaHCO_3$) [156]. A key component in this system was $NaHCO_3$, which has shown to trigger the pH-responsive drug release rapidly in a Lewis rat model. Upon insertion into the slightly acidic skin, PVP dissolved rapidly and $NaHCO_3$ generated CO_2 bubbles within minutes, sequentially allowing the release of the cargo. In addition, Wang et al. reported a self-degradable MN patch, which promoted the generation of acid in the local environment to facilitate sustained delivery of anti-programmed death 1 (anti-PD-1) monoclonal antibody for treatment of melanoma [157]. Each MN was composed of biocompatible HA integrated with NPs made from ethoxypropene-conjugated dextran. Upon piercing into the immune-cell-rich epidermis, the MN delivered NPs to the regional lymph and capillary vessels in the skin. At the same time, the catalase (CAT) and GOx assisted BG oxidation and helped consume undesired H_2O_2 [158–161]. With the GOx/CAT enzymatic system immobilized inside the NPs, the enzyme-mediated generation of gluconic acid promoted the gradual self-dissociation of NPs and resulted in the sustained release of embedded anti-PD-1 monoclonal antibody over a three-day administration period. In addition, treated tumors were remarkably infiltrated by both effector CD8+ and CD4+ T cells. The percentage of CD8+ T cells in the tumor after the MN patch administration was 3-fold of that in the free aPD1 treatment group and 5-fold compared to that in the control MNs or untreated group [162,163] (Fig. 8).

The dysregulation of enzymes expression and activity is implicated in many diseases, which may be leveraged in enzyme-responsive patches for on-demand transdermal drug delivery [52,143,164,165]. Recently, the overexpressed hyaluronidase (HAase) in the tumor microenvironment was applied by Ye et al. for synergistic immunotherapy to enhance antitumor immunity [166]. In this work, 1-methyl-*DL*-tryptophan (1-MT, an inhibitor of indoleamine 2,3-dioxygenase)-modified HA was self-assembled to form immunotherapeutic nanocapsules encapsulating anti-PD-1 antibody [167]. Drug release was triggered by the enzymatic digestion of HA material in the tumor microenvironment. When the resulting MNs were administered to the local tumor site in a B16F10 mouse melanoma model, the system generated an enhanced effective T cell immunity and reduced immuno-suppression.

In another study, a feedback-controlled drug delivery system was engineered for the management of thrombotic diseases [101]. Zhang et al. designed a heparin-conjugated HA (TR-HAHP) matrix with a thrombin-cleavable peptide (GGLVPR|GSGGC) linker. The resulting MNs patch made of TR-HAHP was designed to promptly release heparin triggered by elevated thrombin concentration. Subsequent *in vivo* studies of the TR-HAHP patch demonstrated efficient protection against thrombolytic challenge and long-term thrombosis prevention.

4. Conclusion and outlook

As surveyed above, therapeutic protein delivery through polymeric MN patches has received considerable attention for different applications (Table 1). Currently, there are approximately 23 active and 39 completed National Institutes of Health (NIH) clinical trials related to MNs for treating a variety of diseases, including type 1 diabetes, psoriatic plaques and topical anesthesia [184]. Most studies utilize commercial available hollow MN infusion systems, and a few cases have investigated the effectiveness of using polymeric MN for protein drug delivery. For example, a Phase I study investigating the safety and immunogenicity of the dissolvable MN for the delivery of H1N1, H3N2 and B seasonal influenza virus vaccine strains has been published (ClinicalTrials.gov identifier: NCT02438423) [185]. A coated transdermal MN delivery system has been completed in phase II clinical study for the systemic delivery of a parathyroid hormone-related protein (ClinicalTrials.gov identifier: NCT01674621). A complete Phase I study with a Zosano Pharma PTH coated MN patch was to evaluate the injection site, treatment window and drug dosage and determine the patient preference and adverse effects in postmenopausal women (ClinicalTrials.gov identifier: NCT02478879).

The future success of clinical application relies profoundly on the rational design of the polymeric MN with excellent biocompatibility over both short- and long-term. More and more animal studies have included biocompatibility evaluation upon the usage of polymeric MNs. For example, Noh et al. measured human skin irritation after administration of polycarbonate MNs, concluding that there was little difference in the transient redness after the MN application compared to the control group without treatment [186]. Moreover, the safety of the MN patch has been evaluated in a rhesus macaque non-human primate model and no signs of bleeding, swelling, discharge or other abnormalities were observed in one week after the study [103]. Future studies involve a thorough evaluation of the dermal metabolism of the drug as well as degradation of formulation material and the long-term negative patient adverse effects according to FDA's standards [187]. Moreover, significant efforts regarding MN manufacture should be taken into account to expedite the translation potential, including large-scale fabrication with limited defects, ease of sterilization and enhanced loading capacity to meet versatile applications. The past two decades have witnessed the prosperous development of both innovations and translations of MNs for drug delivery application. With the further combination of fundamental studies and commercialization programs, an accelerating era of MN-mediated protein delivery products is optimistically expected to enhance patients' health and quality of life.

Acknowledgments

This work was supported by the grants from the American Diabetes Association (ADA) (1-15-ACE-21), the JDRF (2-SRA-2016-269-A-N) and the National Science Foundation (1708620) to Z.G.

References

1. Barry BW. Breaching the skin's barrier to drugs. Nat Biotechnol. 2004; 22:165–167. [PubMed: 14755286]
2. Eisenstein M. Something new under the skin. Nat Biotechnol. 2011; 29:107–109. [PubMed: 21301430]
3. Chandrasekhar S, Iyer LK, Panchal JP, Topp EM, Cannon JB, Ranade VV. Micro-arrays and microneedle arrays for delivery of peptides, proteins, vaccines and other applications. Expert Opin Drug Deliv. 2013; 10:1155–1170. [PubMed: 23662940]
4. Prausnitz MR. Microneedles for transdermal drug delivery. Adv Drug Deliv Rev. 2004; 56:581–587. [PubMed: 15019747]
5. Park J-H, Allen MG, Prausnitz MR. Polymer microneedles for controlled-release drug delivery. Pharm Res. 2006; 23:1008–1019. [PubMed: 16715391]
6. Kim Y-C, Park J-H, Prausnitz MR. Microneedles for drug and vaccine delivery. Adv Drug Deliv Rev. 2012; 64:1547–1568. [PubMed: 22575858]
7. McAllister DV, Wang PM, Davis SP, Park JH, Canatella PJ, Allen MG, et al. Microfabricated needles for transdermal delivery of macromolecules and nanoparticles: fabrication methods and transport studies. Proc Natl Acad Sci U S A. 2003; 100:13755–13760. [PubMed: 14623977]
8. Prausnitz MR, Langer R. Transdermal drug delivery. Nat Biotechnol. 2008; 26:1261–1268. [PubMed: 18997767]
9. Kaushik S, Hord AH, Denson DD, McAllister DV, Smitra S, Allen MG, et al. Lack of pain associated with microfabricated microneedles. Anesth Analg. 2001; 92:502–504. [PubMed: 11159258]
10. Kim Y-C, Prausnitz MR. Enabling skin vaccination using new delivery technologies. Drug Deliv Transl Res. 2010; 1:7–12.
11. Raphael AP, Prow TW, Crichton ML, Chen X, Fernando GJP, Kendall MAF. Targeted, needle-free vaccinations in skin using multilayered, densely-packed dissolving microprojection arrays. Small. 2010; 6:1785–1793. [PubMed: 20665628]
12. Sullivan SP, Koutsonanos DG, del Pilar Martin M, Lee JW, Zarnitsyn V, Choi S-O, et al. Dissolving polymer microneedle patches for influenza vaccination. Nat Med. 2010; 16:915–920. [PubMed: 20639891]
13. Kretsos K, Kasting GB. Dermal capillary clearance: physiology and modeling. Skin Pharmacol Physiol. 2005; 18:55–74. [PubMed: 15767767]
14. Lambert PE, Laurent PH. Intradermal vaccine delivery: will new delivery systems transform vaccine administration? Vaccine. 2008; 26:3197–3208. [PubMed: 18486285]
15. Mikszta JA, Laurent PE. Cutaneous delivery of prophylactic and therapeutic vaccines: historical perspective and future outlook. Expert Rev Vaccines. 2008; 7:1329–1339. [PubMed: 18980537]
16. Simon L, Goyal A. Dynamics and control of percutaneous drug absorption in the presence of epidermal turnover. J Pharm Sci. 2009; 98:187–204. [PubMed: 18481307]
17. Harvey AJ, Kaestner SA, Sutter DE, Harvey NG, Mikszta JA, Pettis RJ. Microneedle-based intradermal delivery enables rapid lymphatic uptake and distribution of protein drugs. Pharm Res. 2010; 28:107–116. [PubMed: 20354765]
18. Segura E, Villadangos JA. Antigen presentation by dendritic cells in vivo. Curr Opin Immunol. 2009; 21:105–110. [PubMed: 19342210]
19. Zaba LC, Krueger JG, Lowes MA. Resident and "inflammatory" dendritic cells in human skin. J Invest Dermatol. 2009; 129:302–308. [PubMed: 18685620]
20. Gupta J, Gill HS, Andrews SN, Prausnitz MR. Kinetics of skin resealing after insertion of microneedles in human subjects. J Control Release. 2011; 154:148–155. [PubMed: 21640148]

21. Alarcon JB, Hartley AW, Harvey NG, Mikszta JA. Preclinical evaluation of microneedle technology for intradermal delivery of influenza vaccines. Clin Vaccine Immunol. 2007; 14:375–381. [PubMed: 17329444]
22. Mitragotri S. Immunization without needles. Nat Rev Immunol. 2005; 5:905–916. [PubMed: 16239901]
23. Lee JW, Park J-H, Prausnitz MR. Dissolving microneedles for transdermal drug delivery. Biomaterials. 2008; 29:2113–2124. [PubMed: 18261792]
24. Sullivan SP, Murthy N, Prausnitz MR. Minimally invasive protein delivery with rapidly dissolving polymer microneedles. Adv Mater. 2008; 20:933–938. [PubMed: 23239904]
25. Park J-H, Allen MG, Prausnitz MR. Biodegradable polymer microneedles: fabrication, mechanics and transdermal drug delivery. J Control Release. 2005; 104:51–66. [PubMed: 15866334]
26. Moga KA, Bickford LR, Geil RD, Dunn SS, Pandya AA, Wang Y, et al. Rapidly-dissolvable microneedle patches via a highly scalable and reproducible soft lithography approach. Adv Mater. 2013; 25:5060–5066. [PubMed: 23893866]
27. Lee JW, Han MR, Park JH. Polymer microneedles for transdermal drug delivery. J Drug Target. 2012; 21:211–223.
28. Lee K, Lee CY, Jung H. Dissolving microneedles for transdermal drug administration prepared by stepwise controlled drawing of maltose. Biomaterials. 2011; 32:3134–3140. [PubMed: 21292317]
29. Gupta J, Felner EI, Prausnitz MR. Minimally invasive insulin delivery in subjects with type 1 diabetes using hollow microneedles. Diabetes Technol Ther. 2009; 11:329–337. [PubMed: 19459760]
30. Gill HS, Prausnitz MR. Coating formulations for microneedles. Pharm Res. 2007; 24:1369–1380. [PubMed: 17385011]
31. Kim Y-C, Quan F-S, Compans RW, Kang S-M, Prausnitz MR. Formulation and coating of microneedles with inactivated influenza virus to improve vaccine stability and immunogenicity. J Control Release. 2010; 142:187–195. [PubMed: 19840825]
32. Langer R, Folkman J. Polymers for the sustained release of proteins and other macromolecules. Nature. 1976; 263:797–800. [PubMed: 995197]
33. van der Maaden K, Jiskoot W, Bouwstra J. Microneedle technologies for (trans) dermal drug and vaccine delivery. J Control Release. 2012; 161:645–655. [PubMed: 22342643]
34. Herwadkar A, Banga AK. Peptide and protein transdermal drug delivery. Drug Discov Today Technol. 2012; 9:e147–e154.
35. Wu F, Yang S, Yuan W, Jin T. Challenges and strategies in developing microneedle patches for transdermal delivery of protein and peptide therapeutics. Curr Pharm Biotechnol. 2012; 13:1292–1298. [PubMed: 22201589]
36. Schoellhammer CM, Blankschtein D, Langer R. Skin permeabilization for transdermal drug delivery: recent advances and future prospects. Expert Opin Drug Deliv. 2014; 11:393–407. [PubMed: 24392787]
37. Cevc G, Vierl U. Nanotechnology and the transdermal route: a state of the art review and critical appraisal. J Control Release. 2010; 141:277–299. [PubMed: 19850095]
38. van der Maaden K, Yu H, Sliedregt K, Zwier R, Leboux R, Oguri M, et al. Nanolayered chemical modification of silicon surfaces with ionizable surface groups for pH-triggered protein adsorption and release: application to microneedles. J Mater Chem B. 2013; 1:4466.
39. Guerci B, Sauvanet JP. Subcutaneous insulin: pharmacokinetic variability and glycemic variability. Diabetes Metab. 2005; 31:4S7–4S24. [PubMed: 16389894]
40. White HD, Ahmad AM, Vora JP. Effects of adult growth hormone deficiency and growth hormone replacement on circadian rhythmicity. Minerva Endocrinol. 2003; 28:13–25. [PubMed: 12621360]
41. Yu J, Zhang Y, Ye Y, DiSanto R, Sun W, Ranson D, et al. Microneedle-array patches loaded with hypoxia-sensitive vesicles provide fast glucose-responsive insulin delivery. Proc Natl Acad Sci. 2015; 112:8260–8265. [PubMed: 26100900]
42. Lee JW, Choi S-O, Felner EI, Prausnitz MR. Dissolving microneedle patch for transdermal delivery of human growth hormone. Small. 2011; 7:531–539. [PubMed: 21360810]

43. Leader B, Baca QJ, Golan DE. Protein therapeutics: a summary and pharmacological classification. Nat Rev Drug Discov. 2008; 7:21–39. [PubMed: 18097458]
44. Hawkins MJ, Soon-Shiong P, Desai N. Protein nanoparticles as drug carriers in clinical medicine. Adv Drug Deliv Rev. 2008; 60:876–885. [PubMed: 18423779]
45. Reichert JM. A guide to drug discovery: trends in development and approval times for new therapeutics in the United States. Nat Rev Drug Discov. 2003; 2:695–702. [PubMed: 12951576]
46. Pavlou AK, Reichert JM. Recombinant protein therapeutics? Success rates, market trends and values to 2010. Nat Biotechnol. 2004; 22:1513–1519. [PubMed: 15583654]
47. Yan M, Du J, Gu Z, Liang M, Hu Y, Zhang W, et al. A novel intracellular protein delivery platform based on single-protein nanocapsules. Nat Nanotechnol. 2009; 5:48–53. [PubMed: 19935648]
48. Frokjaer S, Otzen DE. Protein drug stability: a formulation challenge. Nat Rev Drug Discov. 2005; 4:298–306. [PubMed: 15803194]
49. Lu Y, Sun W, Gu Z. Stimuli-responsive nanomaterials for therapeutic protein delivery. J Control Release. 2014; 194:1–19. [PubMed: 25151983]
50. Ye Y, Yu J, Gu Z. Versatile protein nanogels prepared by in situ polymerization. Macromol Chem Phys. 2016; 217:333–343.
51. Mitragotri S, Burke PA, Langer R. Overcoming the challenges in administering biopharmaceuticals: formulation and delivery strategies. Nat Rev Drug Discov. 2014; 13:655–672. [PubMed: 25103255]
52. Sun W, Hu Q, Ji W, Wright G, Gu Z. Leveraging physiology for precision drug delivery. Physiol Rev. 2016; 97:189–225.
53. Ratanji KD, Derrick JP, Dearman RJ, Kimber I. Immunogenicity of therapeutic proteins: influence of aggregation. J Immunotoxicol. 2013; 11:99–109. [PubMed: 23919460]
54. Zhu G, Mallery SR, Schwendeman SP. Stabilization of proteins encapsulated in injectable poly (lactide-*co*-glycolide). Nat Biotechnol. 2000; 18:52–57. [PubMed: 10625391]
55. Rothe A, Power BE, Hudson PJ. Therapeutic advances in rheumatology with the use of recombinant proteins. Nat Clin Pract Rheumatol. 2008; 4:605–614. [PubMed: 18813220]
56. Fukushima K, Yamazaki T, Hasegawa R, Ito Y, Sugioka N, Takada K. Pharmacokinetic and pharmacodynamic evaluation of insulin dissolving microneedles in dogs. Diabetes Technol Ther. 2010; 12:465–474. [PubMed: 20470231]
57. Ito Y, Hasegawa R, Fukushima K, Sugioka N, Takada K. Self-dissolving micropile array chip as percutaneous delivery system of protein drug. Biol Pharm Bull. 2010; 33:683–690. [PubMed: 20410606]
58. Tanner T, Marks R. Delivering drugs by the transdermal route: review and comment. Skin Res Technol. 2008; 14:249–260. [PubMed: 19159369]
59. Zalevsky J, Chamberlain AK, Horton HM, Karki S, Leung IWL, Sproule TJ, et al. Enhanced antibody half-life improves in vivo activity. Nat Biotechnol. 2010; 28:157–159. [PubMed: 20081867]
60. Ito Y, Kashiwara S, Fukushima K, Takada K. Two-layered dissolving microneedles for percutaneous delivery of sumatriptan in rats. Drug Dev Ind Pharm. 2011; 37:1387–1393. [PubMed: 21545233]
61. Karimi M, Sahandi Zangabad P, Baghaee-Ravari S, Ghazadeh M, Mirshekari H, Hamblin MR. Smart nanostructures for cargo delivery: uncaging and activating by light. J Am Chem Soc. 2017; 139:4584–4610. [PubMed: 28192672]
62. Cobo I, Li M, Sumerlin BS, Perrier S. Smart hybrid materials by conjugation of responsive polymers to biomacromolecules. Nat Med. 2014; 14:143–159.
63. Chen W, Tian R, Xu C, Yung BC, Wang G, Liu Y, et al. Microneedle-array patches loaded with dual mineralized protein/peptide particles for type 2 diabetes therapy. Nat Commun. 2017; 8:1777. [PubMed: 29176623]
64. Donnelly RF, Morrow DIJ, Singh TRR, Migalska K, McCarron PA, O'Mahony C, et al. Processing difficulties and instability of carbohydrate microneedle arrays. Drug Dev Ind Pharm. 2009; 35:1242–1254. [PubMed: 19555249]

65. Yang PY, Zou H, Chao E, Sherwood L, Nunez V, Keeney M, et al. Engineering a long-acting, potent GLP-1 analog for microstructure-based transdermal delivery. Proc Natl Acad Sci U S A. 2016; 113:4140–4145. [PubMed: 27035989]
66. Ito Y, Hagiwara E, Saeki A, Sugioka N, Takada K. Feasibility of microneedles for percutaneous absorption of insulin. Eur J Pharm Sci. 2006; 29:82–88. [PubMed: 16828268]
67. Ameri M, Wang X, Maa Y-F. Effect of irradiation on parathyroid hormone PTH(1-34) coated on a novel transdermal microprojection delivery system to produce a sterile product—adhesive compatibility. J Pharm Sci. 2009; 99:2123–2134.
68. Riechmann L, Clark M, Waldmann H, Winter G. Reshaping human antibodies for therapy. Nature. 1988; 332:323–327. [PubMed: 3127726]
69. Imai K, Takaoka A. Comparing antibody and small-molecule therapies for cancer. Nat Rev Cancer. 2006; 6:714–727. [PubMed: 16929325]
70. Gajewski TF, Schreiber H, Fu YX. Innate and adaptive immune cells in the tumor microenvironment. Nat Immunol. 2013; 14:1014–1022. [PubMed: 24048123]
71. Allen TM. Ligand-targeted therapeutics in anticancer therapy. Nat Rev Cancer. 2002; 2:750–763. [PubMed: 12360278]
72. Melero I, Berman DM, Aznar MA, Korman AJ, Perez Gracia JL, Haanen J. Evolving synergistic combinations of targeted immunotherapies to combat cancer. Nat Rev Cancer. 2015; 15:457–472. [PubMed: 26205340]
73. Smyth MJ, Ngiow SF, Ribas A, Teng MW. Combination cancer immunotherapies tailored to the tumour microenvironment. Nat Rev Clin Oncol. 2016; 13:143–158. [PubMed: 26598942]
74. Couzin-Frankel J. Breakthrough of the year 2013. Cancer immunotherapy. Science. 2013; 342:1432–1433. [PubMed: 24357284]
75. Li G, Badkar A, Nema S, Kolli CS, Banga AK. In vitro transdermal delivery of therapeutic antibodies using maltose microneedles. Int J Pharm. 2009; 368:109–115. [PubMed: 18996461]
76. Reichert JM, Rosensweig CJ, Faden LB, Dewitz MC. Monoclonal antibody successes in the clinic. Nat Biotechnol. 2005; 23:1073–1078. [PubMed: 16151394]
77. Weiner GJ. Building better monoclonal antibody-based therapeutics. Nat Rev Cancer. 2015; 15:361–370. [PubMed: 25998715]
78. Beck A, Wurch T, Bailly C, Corvaia N. Strategies and challenges for the next generation of therapeutic antibodies. Nat Rev Immunol. 2010; 10:345–352. [PubMed: 20414207]
79. Leavy O. Therapeutic antibodies: past, present and future. Nat Rev Immunol. 2010; 10:297. [PubMed: 20422787]
80. Chennamsetty N, Voynov V, Kayser V, Helk B, Trout BL. Design of therapeutic proteins with enhanced stability. Proc Natl Acad Sci U S A. 2009; 106:11937–11942. [PubMed: 19571001]
81. Mönkäre J, Reza Nejadnik M, Baccouche K, Romeijn S, Jiskoot W, Bouwstra JA. IgG-loaded hyaluronan-based dissolving microneedles for intradermal protein delivery. J Control Release. 2015; 218:53–62. [PubMed: 26437262]
82. Kenney RT, Frech SA, Muenz LR, Villar CP, Glenn GM. Dose sparing with intra-dermal injection of influenza vaccine. N Engl J Med. 2004; 351:2295–2301. [PubMed: 15525714]
83. Auewarakul P, Kositanont U, Sornsathapornkul P, Tothong P, Kanyok R, Thongcharoen P. Antibody responses after dose-sparing intradermal influenza vaccination. Vaccine. 2007; 25:659–663. [PubMed: 17011678]
84. Belshe RB, Newman FK, Wilkins K, Graham IL, Babusis E, Ewell M, et al. Comparative immunogenicity of trivalent influenza vaccine administered by intradermal or intramuscular route in healthy adults. Vaccine. 2007; 25:6755–6763. [PubMed: 17692438]
85. Rosenberg SA, Yang JC, Restifo NP. Cancer immunotherapy: moving beyond current vaccines. Nat Med. 2004; 10:909–915. [PubMed: 15340416]
86. Kim Y-C, Quan F-S, Yoo D-G, Compans RW, Kang S-M, Prausnitz MR. Improved influenza vaccination in the skin using vaccine coated microneedles. Vaccine. 2009; 27:6932–6938. [PubMed: 19761836]
87. Schumacher TN, Schreiber RD. Neoantigens in cancer immunotherapy. Science. 2015; 348:69–74. [PubMed: 25838375]

88. Glenn GM, Taylor DN, Li X, Frankel S, Montemarano A, Alving CR. Transcutaneous immunization: a human vaccine delivery strategy using a patch. Nat Med. 2000; 6:1403–1406. [PubMed: 11100128]

89. Mikszta JA, Alarcon JB, Brittingham JM, Sutter DE, Pettis RJ, Harvey NG. Improved genetic immunization via micromechanical disruption of skin-barrier function and targeted epidermal delivery. Nat Med. 2002; 8:415–419. [PubMed: 11927950]

90. Kupper TS, Fuhlbrigge RC. Immune surveillance in the skin: mechanisms and clinical consequences. Nat Rev Immunol. 2004; 4:211–222. [PubMed: 15039758]

91. Bennewitz NL, Babensee JE. The effect of the physical form of poly(lactic-*co*-glycolic acid) carriers on the humoral immune response to co-delivered antigen. Biomaterials. 2005; 26:2991–2999. [PubMed: 15603794]

92. Yekaterina Ostapchuk YP. Hyaluronan-binding T regulatory cells in peripheral blood of breast cancer patients. J Clin Cell Immunol. 2015; 06

93. Chen X, Fernando GJP, Crichton ML, Flaim C, Yukiko SR, Fairmaid EJ, et al. Improving the reach of vaccines to low-resource regions, with a needle-free vaccine delivery device and long-term thermostabilization. J Control Release. 2011; 152:349–355. [PubMed: 21371510]

94. Giudice EL, Campbell JD. Needle-free vaccine delivery. Adv Drug Deliv Rev. 2006; 58:68–89. [PubMed: 16564111]

95. Mistilis MJ, Joyce JC, Esser ES, Skountzou I, Compans RW, Bommarius AS, et al. Long-term stability of influenza vaccine in a dissolving microneedle patch. Drug Deliv Transl Res. 2017; 7:195–205. [PubMed: 26926241]

96. Zhu Q, Zarnitsyn VG, Ye L, Wen Z, Gao Y, Pan L, et al. Immunization by vaccine-coated microneedle arrays protects against lethal influenza virus challenge. Proc Natl Acad Sci U S A. 2009; 106:7968–7973. [PubMed: 19416832]

97. Kommareddy S, Baudner BC, Oh S, Kwon S-Y, Singh M, O'Hagan DT. Dissolvable microneedle patches for the delivery of cell-culture-derived influenza vaccine antigens. J Pharm Sci. 2012; 101:1021–1027. [PubMed: 22190403]

98. Weldon WC, Martin MP, Zarnitsyn V, Wang B, Koutsonanos D, Skountzou I, et al. Microneedle vaccination with stabilized recombinant influenza virus hemagglutinin induces improved protective immunity. Clin Vaccine Immunol. 2011; 18:647–654. [PubMed: 21288996]

99. Wendorf JR, Ghartey-Tagoe EB, Williams SC, Enioutina E, Singh P, Cleary GW. Transdermal delivery of macromolecules using solid-state biodegradable microstructures. Pharm Res. 2010; 28:22–30. [PubMed: 20535531]

100. Choi H-J, Yoo D-G, Bondy BJ, Quan F-S, Compans RW, Kang S-M, et al. Stability of influenza vaccine coated onto microneedles. Biomaterials. 2012; 33:3756–3769. [PubMed: 22361098]

101. Zhang Y, Yu J, Wang J, Hanne NJ, Cui Z, Qian C, et al. Thrombin-responsive transcutaneous patch for auto-anticoagulant regulation. Adv Mater. 2017; 29:1604043.

102. DeMuth PC, Li AV, Abbink P, Liu J, Li H, Stanley KA, et al. Vaccine delivery with microneedle skin patches in nonhuman primates. Nat Biotechnol. 2013; 31:1082–1085.

103. Edens C, Collins ML, Goodson JL, Rota PA, Prausnitz MR. A microneedle patch containing measles vaccine is immunogenic in non-human primates. Vaccine. 2015; 33:4712–4718. [PubMed: 25770786]

104. Gill HS, Prausnitz MR. Coated microneedles for transdermal delivery. J Control Release. 2007; 117:227–237. [PubMed: 17169459]

105. Donnelly RF, Raj Singh TR, Woolfson AD. Microneedle-based drug delivery systems: microfabrication, drug delivery, and safety. Drug Deliv. 2010; 17:187–207. [PubMed: 20297904]

106. Chen X, Kask AS, Crichton ML, McNeilly C, Yukiko S, Dong L, et al. Improved DNA vaccination by skin-targeted delivery using dry-coated densely-packed microprojection arrays. J Control Release. 2010; 148:327–333. [PubMed: 20850487]

107. Ma Y, Gill HS. Coating solid dispersions on microneedles via a molten dip-coating method: development and in vitro evaluation for transdermal delivery of a water-insoluble drug. J Pharm Sci. 2014; 103:3621–3630. [PubMed: 25213295]

108. Davidson A, Al-Qallaf B, Das DB. Transdermal drug delivery by coated microneedles: geometry effects on effective skin thickness and drug permeability. Chem Eng Res Des. 2008; 86:1196–1206.
109. Peters EE, Ameri M, Wang X, Maa Y-F, Daddona PE. Erythropoietin-coated ZP-microneedle transdermal system: preclinical formulation, stability, and delivery. Pharm Res. 2012; 29:1618–1626. [PubMed: 22258935]
110. Cormier M, Johnson B, Ameri M, Nyam K, Libiran L, Zhang DD, et al. Transdermal delivery of desmopressin using a coated microneedle array patch system. J Control Release. 2004; 97:503–511. [PubMed: 15212882]
111. Kommareddy S, Baudner BC, Bonificio A, Gallorini S, Palladino G, Determan AS, et al. Influenza subunit vaccine coated microneedle patches elicit comparable immune responses to intramuscular injection in guinea pigs. Vaccine. 2013; 31:3435–3441. [PubMed: 23398932]
112. Widera G, Johnson J, Kim L, Libiran L, Nyam K, Daddona PE, et al. Effect of delivery parameters on immunization to ovalbumin following intracutaneous administration by a coated microneedle array patch system. Vaccine. 2006; 24:1653–1664. [PubMed: 16246466]
113. Gill HS, Kang S-M, Quan F-S, Compans RW. Cutaneous immunization: an evolving paradigm in influenza vaccines. Expert Opin Drug Deliv. 2014; 11:615–627. [PubMed: 24521050]
114. Matriano JA, Cormier M, Johnson J, Young WA, Buttery M, Nyam K, et al. Macroflux microprojection array patch technology: a new and efficient approach for intracutaneous immunization. Pharm Res. 2002; 19:63–70. [PubMed: 11837701]
115. Andrianov AK, DeCollibus DP, Gillis HA, Kha HH, Marin A, Prausnitz MR, et al. Poly[di(carboxylatophenoxy)phosphazene] is a potent adjuvant for intradermal immunization. Proc Natl Acad Sci U S A. 2009; 106:18936–18941. [PubMed: 19864632]
116. DeMuth PC, Moon JJ, Suh H, Hammond PT, Irvine DJ. Releasable layer-by-layer assembly of stabilized lipid nanocapsules on microneedles for enhanced transcutaneous vaccine delivery. ACS Nano. 2012; 6:8041–8051. [PubMed: 22920601]
117. Su X, Kim BS, Kim SR, Hammond PT, Irvine DJ. Layer-by-layer-assembled multilayer films for transcutaneous drug and vaccine delivery. ACS Nano. 2009; 3:3719–3729. [PubMed: 19824655]
118. Lynn DM, Langer R. Degradable Poly(beta-amino esters): Synthesis, Characterization And Self-Assembly with Plasmid DNA. J Am Chem Soc. 2000; 122:10761–10768.
119. Saurer EM, Flessner RM, Sullivan SP, Prausnitz MR, Lynn DM. Layer-by-layer assembly of DNA- and protein-containing films on microneedles for drug delivery to the skin. Biomacromolecules. 2010; 11:3136–3143. [PubMed: 20942396]
120. Zeng Q, Gammon JM, Tostanoski LH, Chiu YC, Jewell CM. In vivo expansion of melanoma-specific T cells using microneedle arrays coated with immune-polyelectrolyte multilayers. ACS Biomater Sci Eng. 2017; 3:195–205. [PubMed: 28286864]
121. Hong X, Wei L, Wu F, Wu Z, Chen L, Liu Z, et al. Dissolving and biodegradable microneedle technologies for transdermal sustained delivery of drug and vaccine. Drug Des Devel Ther. 2013; 7:945–952.
122. An M, Liu H. Dissolving microneedle arrays for transdermal delivery of amphiphilic vaccines. Small. 2017; 13
123. Miyano T, Tobinaga Y, Kanno T, Matsuzaki Y, Takeda H, Wakui M, et al. Sugar micro needles as transdermic drug delivery system. Biomed Microdevices. 2005; 7:185–188. [PubMed: 16133805]
124. Chen M-C, Ling M-H, Lai K-Y, Pramudityo E. Chitosan microneedle patches for sustained transdermal delivery of macromolecules. Biomacromolecules. 2012; 13:4022–4031. [PubMed: 23116140]
125. Chu LY, Choi S-O, Prausnitz MR. Fabrication of dissolving polymer microneedles for controlled drug encapsulation and delivery: bubble and pedestal microneedle designs. J Pharm Sci. 2010; 99:4228–4238. [PubMed: 20737630]
126. Kumar V, Banga AK. Modulated iontophoretic delivery of small and large molecules through microchannels. Int J Pharm. 2012; 434:106–114. [PubMed: 22633929]
127. Kim JD, Kim M, Yang H, Lee K, Jung H. Droplet-born air blowing: novel dissolving microneedle fabrication. J Control Release. 2013; 170:430–436. [PubMed: 23742882]

128. Martin CJ, Allender CJ, Brain KR, Morrissey A, Birchall JC. Low temperature fabrication of biodegradable sugar glass microneedles for transdermal drug delivery applications. J Control Release. 2012; 158:93–101. [PubMed: 22063007]

129. Ito Y, Ohashi Y, Shiroyama K, Sugioka N, Takada K. Self-dissolving micropiles for the percutaneous absorption of recombinant human growth hormone in rats. Biol Pharm Bull. 2008; 31:1631–1633. [PubMed: 18670103]

130. Migalska K, Morrow DIJ, Garland MJ, Thakur R, Woolfson AD, Donnelly RF. Laser-engineered dissolving microneedle arrays for transdermal macromolecular drug delivery. Pharm Res. 2011; 28:1919–1930. [PubMed: 21437789]

131. Pattani A, McKay PF, Garland MJ, Curran RM, Migalska K, Cassidy CM, et al. Microneedle mediated intradermal delivery of adjuvanted recombinant HIV-1 CN54gp140 effectively primes mucosal boost inoculations. J Control Release. 2012; 162:529–537. [PubMed: 22960496]

132. Ling M-H, Chen M-C. Dissolving polymer microneedle patches for rapid and efficient transdermal delivery of insulin to diabetic rats. Acta Biomater. 2013; 9:8952–8961. [PubMed: 23816646]

133. Fukushima K, Ise A, Morita H, Hasegawa R, Ito Y, Sugioka N, et al. Two-layered dissolving microneedles for percutaneous delivery of peptide/protein drugs in rats. Pharm Res. 2010; 28:7–21. [PubMed: 20300802]

134. Vora LK, Donnelly RF, Larraneta E, Gonzalez-Vazquez P, Thakur RRS, Vavia PR. Novel bilayer dissolving microneedle arrays with concentrated PLGA nano-microparticles for targeted intradermal delivery: proof of concept. J Control Release. 2017; 265:93–101. [PubMed: 29037785]

135. DeMuth PC, Min Y, Irvine DJ, Hammond PT. Implantable silk composite microneedles for programmable vaccine release kinetics and enhanced immunogenicity in transcutaneous immunization. Adv Healthc Mater. 2014; 3:47–58. [PubMed: 23847143]

136. Tsioris K, Raja WK, Pritchard EM, Panilaitis B, Kaplan DL, Omenetto FG. Fabrication of silk microneedles for controlled-release drug delivery. Adv Funct Mater. 2012; 22:330–335.

137. Di J, Yao S, Ye Y, Cui Z, Yu J, Ghosh TK, et al. Stretch-triggered drug delivery from wearable elastomer films containing therapeutic depots. ACS Nano. 2015; 9:9407–9415. [PubMed: 26258579]

138. Yang S, Wu F, Liu J, Fan G, Welsh W, Zhu H, et al. Phase-transition microneedle patches for efficient and accurate transdermal delivery of insulin. Adv Funct Mater. 2015; 25:4633–4641.

139. Ye Y, Wang C, Zhang X, Hu Q, Zhang Y, Liu Q, et al. A melanin-mediated cancer immunotherapy patch. Sci Immunol. 2017; 2

140. Zaric M, Lyubomska O, Touzelet O, Poux C, Al-Zahrani S, Fay F, et al. Skin dendritic cell targeting via microneedle arrays laden with antigen-encapsulated poly-D,L-lactide-*co*-glycolide nanoparticles induces efficient antitumor and antiviral immune responses. ACS Nano. 2013; 7:2042–2055. [PubMed: 23373658]

141. Kim M, Jung B, Park J-H. Hydrogel swelling as a trigger to release biodegradable polymer microneedles in skin. Biomaterials. 2012; 33:668–678. [PubMed: 22000788]

142. Yu J, Zhang Y, Kahkoska AR, Gu Z. Bioresponsive transcutaneous patches. Curr Opin Biotechnol. 2017; 48:28–32. [PubMed: 28292673]

143. Lu Y, Aimetti AA, Langer R, Gu Z. Bioresponsive materials. Nat Rev Mater. 2016; 2:16075.

144. Mahapatro A, Singh DK. Biodegradable nanoparticles are excellent vehicle for site directed in-vivo delivery of drugs and vaccines. J Nanobiotechnol. 2011; 9:55.

145. Taghizadeh B, Taranejoo S, Monemian SA, Salehi Moghaddam Z, Daliri K, Derakhshankhah H, et al. Classification of stimuli-responsive polymers as anticancer drug delivery systems. Drug Deliv. 2015; 22:145–155. [PubMed: 24547737]

146. Mura S, Nicolas J, Couvreur P. Stimuli-responsive nanocarriers for drug delivery. Nat Mater. 2013; 12:991–1003. [PubMed: 24150417]

147. de Las Heras Alarcon C, Pennadam S, Alexander C. Stimuli responsive polymers for biomedical applications. Chem Soc Rev. 2005; 34:276–285. [PubMed: 15726163]

148. Peer D, Karp JM, Hong S, Farokhzad OC, Margalit R, Langer R. Nanocarriers as an emerging platform for cancer therapy. Nat Nanotechnol. 2007; 2:751–760. [PubMed: 18654426]

149. Park J-H, Choi S-O, Kamath R, Yoon Y-K, Allen MG, Prausnitz MR. Polymer particle-based micromolding to fabricate novel microstructures. Biomed Microdevices. 2006; 9:223–234.

150. Stuart MAC, Huck WTS, Genzer J, Müller M, Ober C, Stamm M, et al. Emerging applications of stimuli-responsive polymer materials. Nat Mater. 2010; 9:101–113. [PubMed: 20094081]

151. Ye Y, Yu J, Wang C, Nguyen N-Y, Walker GM, Buse JB, et al. Microneedles integrated with pancreatic cells and synthetic glucose-signal amplifiers for smart insulin delivery. Adv Mater. 2016; 28:3115–3121. [PubMed: 26928976]

152. Hu X, Yu J, Qian C, Lu Y, Kahkoska AR, Xie Z, et al. H2O2-responsive vesicles integrated with transcutaneous patches for glucose-mediated insulin delivery. ACS Nano. 2017; 11:613–620. [PubMed: 28051306]

153. Yu J, Qian C, Zhang Y, Cui Z, Zhu Y, Shen Q, et al. Hypoxia and H2O2 dual-sensitive vesicles for enhanced glucose-responsive insulin delivery. Nano Lett. 2017; 17:733–739. [PubMed: 28079384]

154. Skidmore RA, Flowers FP. Nonmelanoma skin cancer. Med Clin North Am. 1998; 82:1309–1323. [PubMed: 9889750]

155. Kim NW, Lee MS, Kim KR, Lee JE, Lee K, Park JS, et al. Polyplex-releasing microneedles for enhanced cutaneous delivery of DNA vaccine. J Control Release. 2014; 179:11–17. [PubMed: 24462900]

156. Ke C-J, Lin Y-J, Hu Y-C, Chiang W-L, Chen K-J, Yang W-C, et al. Multidrug release based on microneedle arrays filled with pH-responsive PLGA hollow microspheres. Biomaterials. 2012; 33:5156–5165. [PubMed: 22484044]

157. Wang C, Ye Y, Hochu GM, Sadeghifar H, Gu Z. Enhanced cancer immunotherapy by microneedle patch-assisted delivery of anti-PD1 antibody. Nano Lett. 2016; 16:2334–2340. [PubMed: 26999507]

158. Gu Z, Dang TT, Ma M, Tang BC, Cheng H, Jiang S, et al. Glucose-responsive microgels integrated with enzyme nanocapsules for closed-loop insulin delivery. ACS Nano. 2013; 7:6758–6766. [PubMed: 23834678]

159. Gu Z, Aimetti AA, Wang Q, Dang TT, Zhang Y, Veiseh O, et al. Injectable nano-network for glucose-mediated insulin delivery. ACS Nano. 2013; 7:4194–4201. [PubMed: 23638642]

160. Zhang Y, Liu Q, Yu J, Yu S, Wang J, Qiang L, et al. Locally induced adipose tissue browning by microneedle patch for obesity treatment. ACS Nano. 2017; 11:9223–9230. [PubMed: 28914527]

161. Chen Z, Wang J, Sun W, Archibong E, Kahkoska AR, Zhang X, et al. Synthetic beta cells for fusion-mediated dynamic insulin secretion. Nat Chem Biol. 2018; 14:86–93. [PubMed: 29083418]

162. Dobrovolskaia MA, McNeil SE. Immunological properties of engineered nanomaterials. Nat Nanotechnol. 2007; 2:469–478. [PubMed: 18654343]

163. Curran MA, Montalvo W, Yagita H, Allison JP. PD-1 and CTLA-4 combination blockade expands infiltrating T cells and reduces regulatory T and myeloid cells within B16 melanoma tumors. Proc Natl Acad Sci. 2010; 107:4275–4280. [PubMed: 20160101]

164. Lee MR, Baek KH, Jin HJ, Jung YG, Shin I. Targeted enzyme-responsive drug carriers: studies on the delivery of a combination of drugs. Angew Chem. 2004; 43:1675–1678. [PubMed: 15038034]

165. Hu Q, Katti PS, Gu Z. Enzyme-responsive nanomaterials for controlled drug delivery. Nanoscale. 2014; 6:12273–12286. [PubMed: 25251024]

166. Ye Y, Wang J, Hu Q, Hochu GM, Xin H, Wang C, et al. Synergistic transcutaneous immunotherapy enhances antitumor immune responses through delivery of checkpoint inhibitors. ACS Nano. 2016; 10:8956–8963. [PubMed: 27599066]

167. Rosenberg SA. Decade in review-cancer immunotherapy: entering the mainstream of cancer treatment. Nat Rev Clin Oncol. 2014; 11:630–632. [PubMed: 25311350]

168. Pearton M, Kang S-M, Song J-M, Kim Y-C, Quan F-S, Anstey A, et al. Influenza virus-like particles coated onto microneedles can elicit stimulatory effects on Langerhans cells in human skin. Vaccine. 2010; 28:6104–6113. [PubMed: 20685601]

169. Ameri M, Fan SC, Maa Y-F. Parathyroid hormone PTH(1-34) formulation that enables uniform coating on a novel transdermal microprojection delivery system. Pharm Res. 2009; 27:303–313. [PubMed: 20013035]

170. Chen X, Prow TW, Crichton ML, Jenkins DW, Roberts MS, Frazer IH, et al. Dry-coated microprojection array patches for targeted delivery of immunotherapeutics to the skin. J Control Release. 2009; 139:212–220. [PubMed: 19577597]

171. Marin A, Andrianov AK. Carboxymethylcellulose-chitosan-coated microneedles with modulated hydration properties. J Appl Polym Sci. 2011; 121:395–401.

172. Andrianov AK, Marin A, DeCollibus DP. Microneedles with intrinsic immunoadjuvant properties: microfabrication, protein stability, and modulated release. Pharm Res. 2011; 28:58–65. [PubMed: 20372988]

173. Han M, Kim DK, Kang SH, Yoon H-R, Kim B-Y, Lee SS, et al. Improvement in antigen-delivery using fabrication of a grooves-embedded microneedle array. Sensors Actuators B Chem. 2009; 137:274–280.

174. Jin J, Reese V, Coler R, Carter D, Rolandi M. Chitin microneedles for an easy-to-use tuberculosis skin test. Adv Healthc Mater. 2014; 3:349–353. [PubMed: 23983170]

175. Ito Y, Murakami A, Maeda T, Sugioka N, Takada K. Evaluation of self-dissolving needles containing low molecular weight heparin (LMWH) in rats. Int J Pharm. 2008; 349:124–129. [PubMed: 17826015]

176. Ito Y, Hagiwara E, Saeki A, Sugioka N, Takada K. Sustained-release self-dissolving micropiles for percutaneous absorption of insulin in mice. J Drug Target. 2007; 15:323–326. [PubMed: 17541840]

177. Ito Y, Ohashi Y, Saeki A, Sugioka N, Takada K. Antihyperglycemic effect of insulin from self-dissolving micropiles in dogs. Chem Pharm Bull. 2008; 56:243–246. [PubMed: 18310929]

178. Ito Y, Saeki A, Shiroyama K, Sugioka N, Takada K. Percutaneous absorption of interferon-alpha by self-dissolving micropiles. J Drug Target. 2008; 16:243–249. [PubMed: 18365886]

179. Ito Y, Yoshimitsu J, Shiroyama K, Sugioka N, Takada K. Self-dissolving microneedles for the percutaneous absorption of EPO in mice. J Drug Target. 2006; 14:255–261. [PubMed: 16882545]

180. Matsuo K, Hirobe S, Yokota Y, Ayabe Y, Seto M, Quan Y-S, et al. Transcutaneous immunization using a dissolving microneedle array protects against tetanus, diphtheria, malaria, and influenza. J Control Release. 2012; 160:495–501. [PubMed: 22516091]

181. Chu LY, Prausnitz MR. Separable arrowhead microneedles. J Control Release. 2011; 149:242–249. [PubMed: 21047538]

182. Bediz B, Korkmaz E, Khilwani R, Donahue C, Erdos G, Falo LD Jr, et al. Dissolvable microneedle arrays for intradermal delivery of biologics: fabrication and application. Pharm Res. 2014; 31:117–135. [PubMed: 23904139]

183. Lee H, Choi TK, Lee YB, Cho HR, Ghaffari R, Wang L, et al. A graphene-based electrochemical device with thermoresponsive microneedles for diabetes monitoring and therapy. Nat Nanotechnol. 2016; 11:566–572. [PubMed: 26999482]

184. Ita K. Transdermal delivery of drugs with microneedles—potential and challenges. Pharmaceutics. 2015; 7:90–105. [PubMed: 26131647]

185. Rouphael NG, Paine M, Mosley R, Henry S, McAllister DV, Kalluri H, et al. The safety, immunogenicity, and acceptability of inactivated influenza vaccine delivered by microneedle patch (TIV-MNP 2015): a randomised, partly blinded, placebo-controlled, phase 1 trial. Lancet. 2017; 390:649–658. [PubMed: 28666680]

186. Noh Y-W, Kim T-H, Baek J-S, Park H-H, Lee SS, Han M, et al. In vitro characterization of the invasiveness of polymer microneedle against skin. Int J Pharm. 2010; 397:201–205. [PubMed: 20619328]

187. Ando HY, Ho NF, Higuchi WI. Skin as an active metabolizing barrier I: theoretical analysis of topical bioavailability. J Pharm Sci. 1977; 66:1525–1528. [PubMed: 915724]

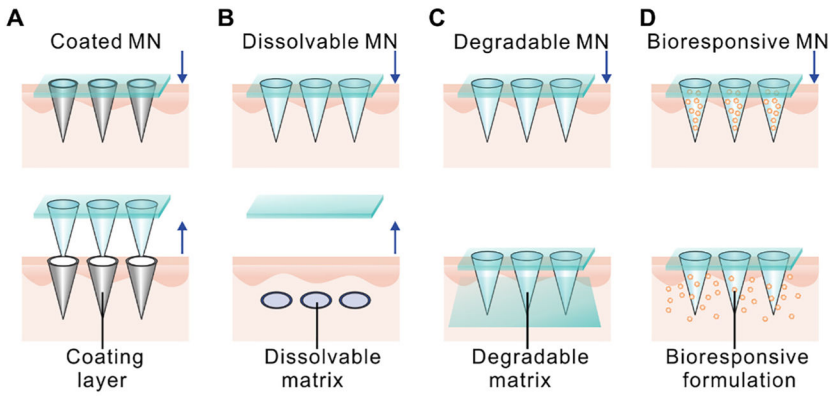

Fig. 1.

Representative types of polymeric MNs for protein delivery. A) Solid MNs coated with polymeric drug formulation on the MNs surface for direct delivery. B) Dissolvable polymeric MNs that remain in the skin and dissolve to deliver the drug encapsulated within. C) Degradable polymeric MNs that remain in the skin and degrade over time. Drug delivery occurs *via* passive diffusion or degradation of the polymeric matrix. D) Bioresponsive polymeric MNs. Drug release is dependent on the degradation or dissociation of MN matrix and/or formulations from the MN matrix.

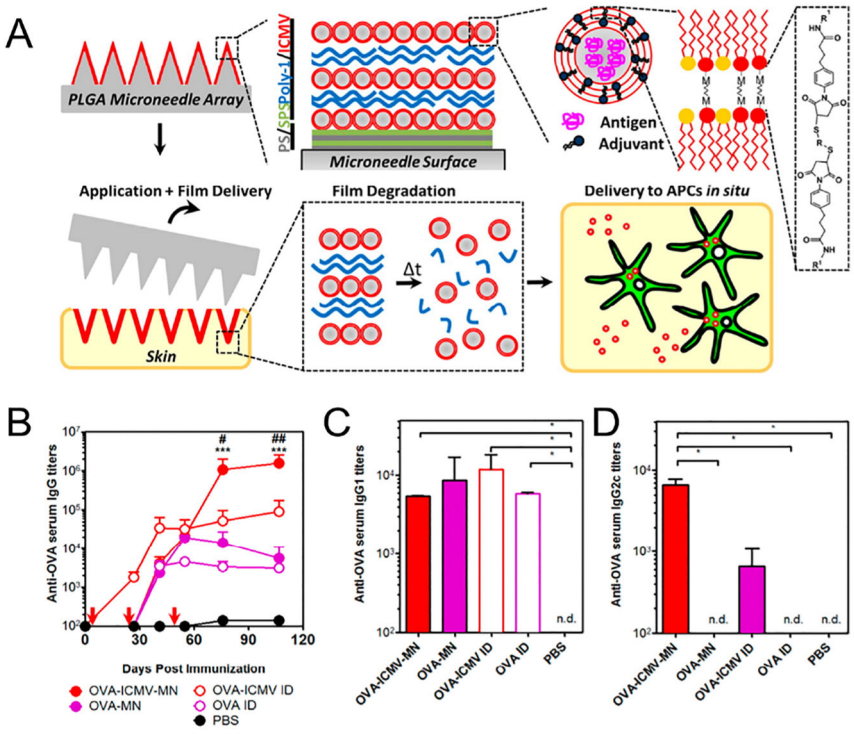

Fig. 2.

A) Schematic illustration of multilayers deposited onto the PLGA MN surfaces. MNs transfer coatings into the skin as an initiation of adaptive immunity. B) Anti-OVA IgG titers in serum over time with MN-based and control immunizations on days 0, 28, and 56. Quantification of C) anti-OVA IgG1 and D) IgG2c subtypes in serum at day 107. Adapted with permission from Ref [116].

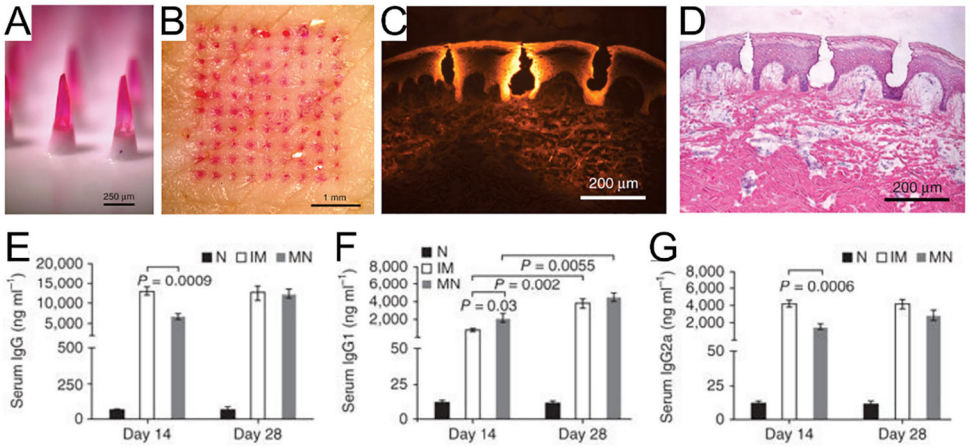

Fig. 3.

A) Side view of dissolvable polymeric MNs. B) Top view of porcine cadaver skin after insertion and removal of MNs with encapsulated sulforhodamine. C) Fluorescence image of pig skin cross section after insertion of one MNs. D) Brightfield image of the skin section with hematoxylin and eosin staining. Quantification of serum influenza-specific E) IgG titers F) IgG1 titers G) IgG2a titers at the indicated days after immunization. Mice were immunized intramuscularly with inactivated influenza virus or *via* an MN patch encapsulating the same amount of virus.

Adapted with permission from Ref [12].

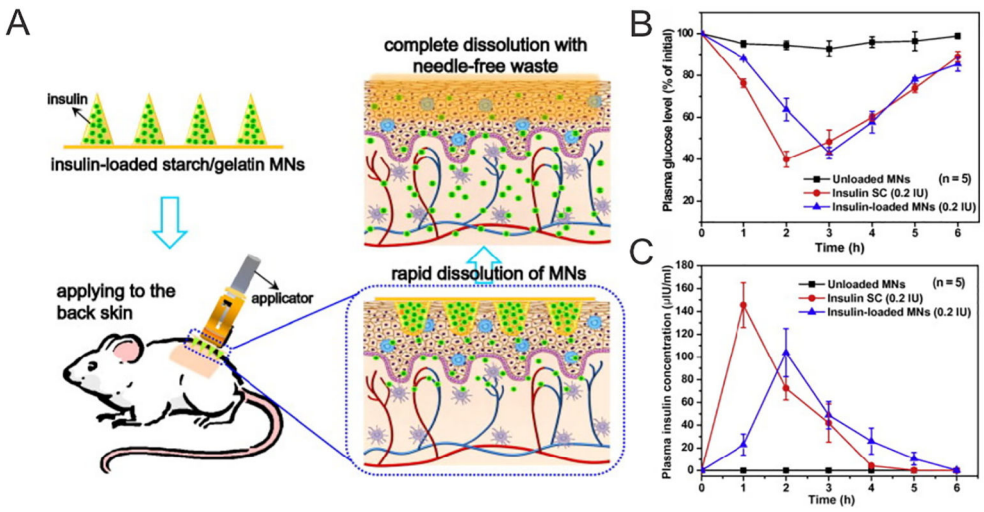

Fig. 4.

A) Schematic illustration of transdermal delivery of insulin using starch/gelatin MNs, which could rapidly dissolve in the skin to release encapsulated insulin. B) Plasma glucose levels and C) plasma insulin concentrations of diabetic rats after administration of control and insulin-loaded MNs.

Adapted with permission from Ref [132].

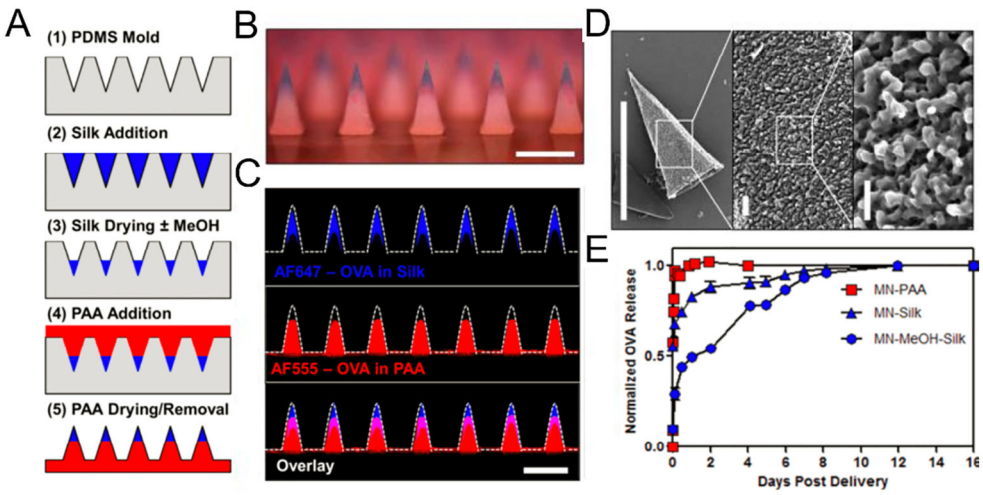

Fig. 5.

Fabrication and characterizations of silk/PAA composite MNs. A) Schematic of MN fabrication. B) Optical micrograph of silk/PAA MN array with silk (blue) in the tips and PAA (red) in the pedestals (scale bar 500 μm). C) Confocal micrographs of composite MNs (scale bar 500 μm). D) SEM micrographs of a single silk tip following 30 s exposure to water. Micrographs show the MN tip structure and silk hydrogel structure (left, scale bar 500 μm, center, scale bar 20 μm, and right, scale bar 5 μm). E) Quantitative analysis of programmed release profiles of fluorescent OVA from silk and PAA portions of the MNs over time.

Adapted with permission from Ref [135].

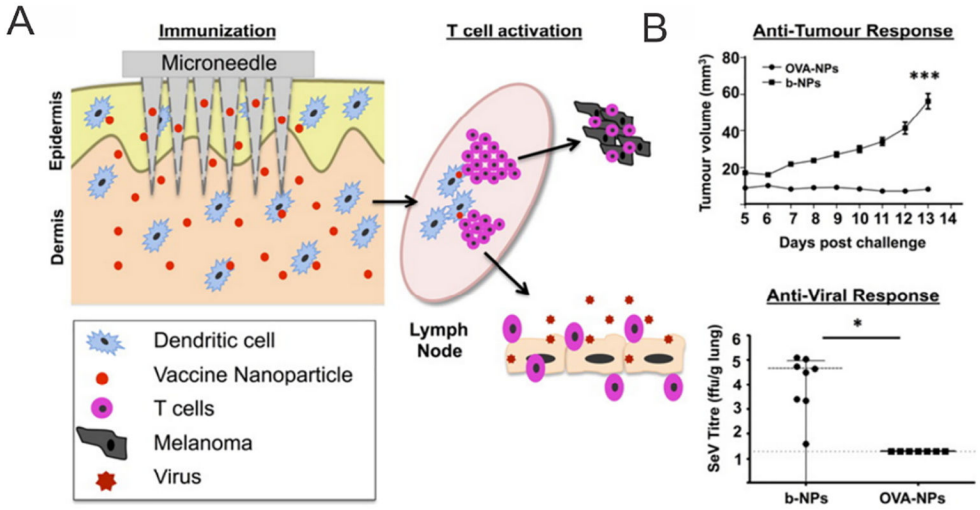

Fig. 6.

A) Schematic of dissolvable MN arrays laden with antigen-loaded NPs to increase vaccine immunogenicity by targeting antigen specifically to DC networks within the skin. B) The antigen-encapsulated NP vaccination *via* MNs generated robust antigen-specific cellular immune responses in mice.

Adapted with permission from Ref [140].

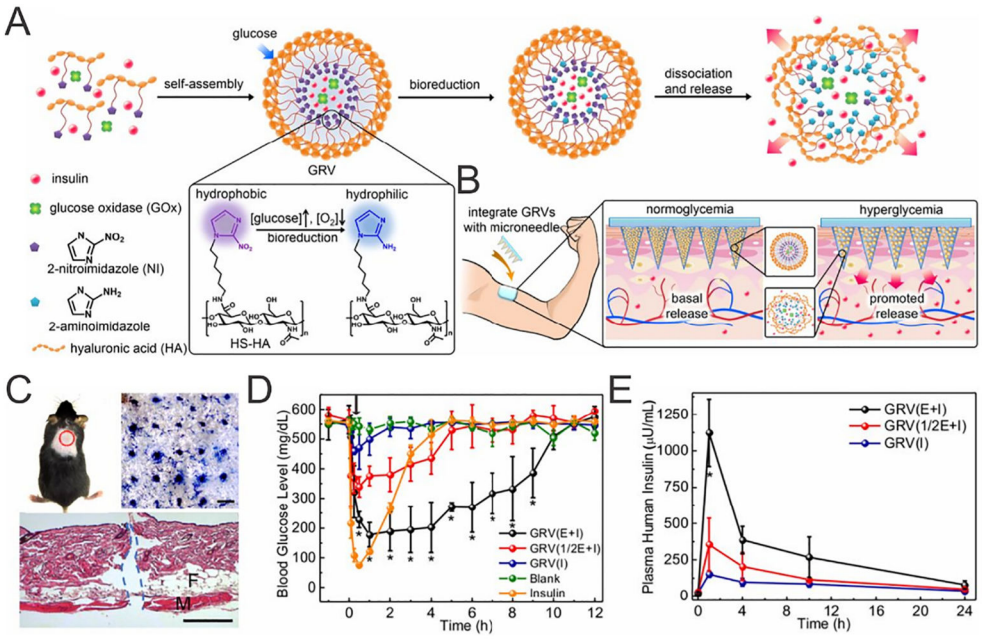

Fig. 7.

A) Schematic of the smart insulin patch composed of HA and GRVs composed of HA. B) Formation and mechanism of glucose-responsive MN patch. C) The indicated mouse skin was applied with an MN-array patch (Scale bar: top right 500 μm, bottom 100 μm). D) *In vivo* BG level changes E) and plasma human insulin concentrations in diabetic mice after indicated treatments.

Adapted with permission from Ref [41].

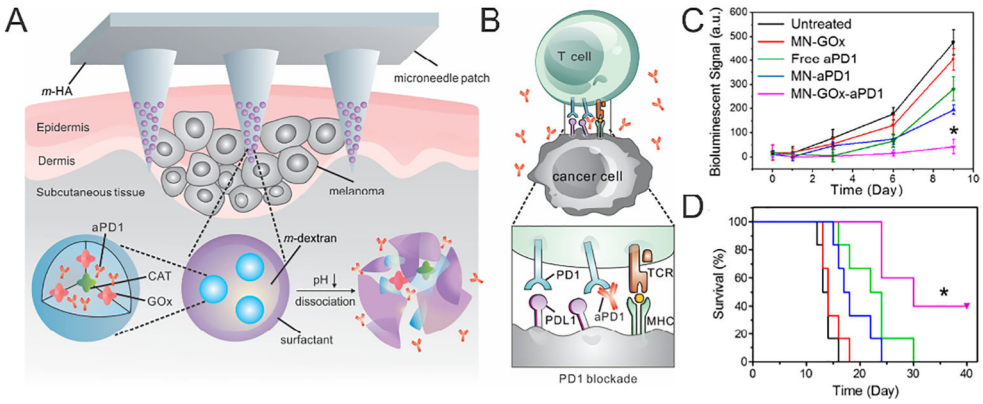

Fig. 8.

A) Schematic of the anti-PD-1 antibody delivery by an MN patch loaded with self-dissociated NPs. B) The blockade of PD-1 by anti-PD-1 antibody activates the immune system to destroy cancer cells. C) Quantified tumor signals according to *in vivo* bioluminescence imaging of the B16F10 tumors in different treatment groups. D) Kaplan-Meier survival curves for the treated mice.

Adapted with permission from Ref [157].

Table 1

Representative polymeric MNs for protein delivery.

MN type	Polymer matrix	Protein drug
Coated MN	Carboxymethylcellulose	H1N1 hemagglutination [100]; recombinant trimeric soluble influenza hemagglutinin [98]; influenza virus-like particle [168]
	Sucrose	Ovalbumin [112]
	Polysorbate 20	Desmopressin [110]; parathyroid hormone [67,169]
	Sodium poly(styrene sulfonate)	Bovine pancreatic ribonuclease [119]; ovalbumin [170]
	Polyethylene/polyisobutylene	Ovalbumin [114]
	Carboxymethylcellulose/chitosan	Bovine serum albumin [171]
	Poly di(carboxylatophenoxy) phosphazene	Horseradish peroxidase [172]; goat-anti-mouse IgG [173]; hepatitis B surface antigen [115]
Dissolvable/degradable MN	Carboxymethylcellulose/trehalose	Human growth hormone [42]
	Carboxymethylcellulose	Bovine serum albumin [23]; lysozyme [23]
	Chitin	Tuberculin [174]
	Chondroitin sulfate	Erythropoietin [56,57]; heparin [175]; insulin [176,177]
	Chondroitin sulfate/dextran	Interferon-α [178]
	Dextran	Erythropoietin [179]; heparin [175]; human growth hormone [129,133]; desmopressin
	Dextrin/polypropylene	Insulin [66]
	Fibroin	Horseradish peroxidase [136]
	Galactose	Bovine serum albumin [64]
	Hyaluronic acid	Influenza hemagglutinin [180]; sumatriptan [60]; humanized monoclonal IgG1 [81]
	Maltose	Biotinylated anti-human IgG [75]
	Poly-L-lactic acid	Bovine serum albumin; HIV antigen [131]; glucagon-like peptide-1 [63,65]
	Poly(lactic-*co*-glycolic acid)/carboxymethylcellulose	Bovine serum albumin [5]
	Poly(methylvinylethercomaleic acid)	Insulin [130]
	Poly(vinyl alcohol)	Recombinant protective antigen; bovine serum albumin [99]
	Poly(vinylpyrrolidone)	Sulforhodamine B; inactivated influenza virus [12,24,181]; hemagglutinin protein [12]; ovalbumin [182]
	Starch/gelatin	Insulin [132]; leuprolide acetate [60]
	Silk/poly(acrylic acid)	Ovalbumin [135]
Bioresponsive MN	Hyaluronic acid	Insulin [41,151]; anti-PD-1 antibody [166]
	Hyaluronic acid/dextran	Anti-PD-1; anti-CTLA-4 antibody [157]
	Hyaluronic acid/poly(ethylene glycol)	Insulin [152,153]
	Poly(vinyl pyrrolidone)	Common drugs [183]
	Alginate	Glucagon-like peptide-1 [63]